# DYNAMIC EARTH PRESSURES ON RIGID WALLS ROTATING ABOUT THE BASE

Mehmet A, Sherif (I)
Yung-Show Fang (II)
Presenting Author: Mehmet A. Sherif

## SUMMARY

This paper presents the results of an experimental investigation of dynamic active stress distribution as a function of accelerations behind a rigid retaining wall rotating about its base. The investigation reveals that the dynamic active stress distribution is non-linear and that the non-linearity increases with increasing acceleration levels. Design curves are proposed to enable the practicing engineer to determine the magnitude and distribution of dynamic active stresses exerted against such walls as a function of acceleration and backfill soil density.

## I. INTRODUCTION

Knowledge of the dynamic stresses exerted against retaining structures of all types is fundamental to their safe and economical design. In the recent past, several analytical and experimental investigations have been undertaken to provide information about lateral stresses (Ref. 1,2,3,4,5,6,7,8, and 9). In spite of these extensive earlier studies, there still remain conflicting opinions regarding the nature and magnitude of the dynamic stresses exerted against retaining structures and the variation of these stresses as a function of both wall movement and acceleration levels. In this paper the authors report on the total stress distribution (static and dynamic) behind a wall rotating about its base and the point of application of the resultant force from the base as a function of acceleration. All the experiments reported in this study were conducted in the University of Washington shaking table-retaining wall system, which is described briefly herein.

## II. INSTRUMENTATION: SHAKING TABLE-RETAINING WALL ASSEMBLY USED IN THIS STUDY

The investigations described in this paper were conducted in a unique shaking table-retaining wall test system, which is shown schematically in Fig. 1. The table is designed to move in one direction. The entire system consists of four components: (1) shaking table and soil box, (2) loading and control units, (3) retaining wall, and (4) data acquisition system as described below.

---

(I) Professor of Civil Engineering and Adjunct Professor of Quaternary Research, University of Washington, Seattle, WA, U.S.A.
(II) Graduate Student of Civil Engineering, University of Washington, Seattle, WA, U.S.A.

1. Shaking Table and Soil Box

The table is 10 ft. long, 8 ft. wide, 7-5/8 in. deep, and is made of steel. It consists of an upper plate 1-1/4 in. thick, a 1-3/8 in. thick lower plate, and 5 in. deep channels forming a grid between the upper and lower plates. A rigid soil box 8 ft. long, 6 ft. wide, and 4 ft. high is built on the shaking table. Both side walls of the box are made of 1/2 in. thick transparent plexiglass through which the behavior of the backfill can be observed. The end wall that sits opposite to the model retaining wall is made of 1/2 in. thick aluminum plates. The bottom of the soil box is covered with a layer of Safety-Walk in order provide adequate friction between the soil and the base of the box.

The shaking table is supported by seven Thomson Roundway bearings. These bearings move on two 1-in. diameter Roundway shafts, which are mounted on the Roundway supports. The shafts and supports are carefully aligned so that all bearings work effectively and simultaneously. The bearings are soaked in oil containers to minimize possible wear due to continuous operation. The combined weight of the table and the empty soil box is 9,100 lbs. The total weight of the shaking table and box fully loaded with sand is 26,000 lbs.

2. Loading and Control Units

An MTS Model 903.73 is used for exciting the shaking table. This system consists of a hydraulic power supply and an actuator. The hydraulic power supply model MTS 503.03 provides a maximum output flow capacity of 20 gpm and an operating pressure of 3,000 psi. The MTS 204.23 is equipped with an LVDT and a servo-valve and has the capacity to produce a maximum stroke of ± 3 in. The maximum static and dynamic force ratings for the actuator are 14,700 lbs. and 12,000 lbs., respectively. The MTS 483.02 is used to regulate the shaking table movement under both stroke and load controls and is capable of generating various loading functions, including earthquake-type excitation.

3. Model Retaining Wall

The movable model retaining wall and its driving system are shown in Fig. 2. The main frame, which includes the center wall, is made of structural aluminum and, for the purposes of this study, was designed to have high flexural stiffness allowing maximum wall deflection of 0.05 mm.

The center wall is 3 ft. 4 in. wide, 3 ft. 5 in. high, and 5 in. thick, and is attached to the main body of the wall frame by means of three horizontal and one vertical load cells and a unidirectional roller located at the wall's bottom. Six diaphragm-type Kulite VM-750 soil pressure transducers are mounted on the center line of the wall surface at different depths (see Fig. 3) in order to measure the soil pressures against the center wall. To eliminate or minimize the side-wall friction from adversely affecting the accuracy of the experimental data, only the center wall is instrumented with pressure transducers and load cells. The wall can undergo several types of movements: (a) rotation about the base, (b) rotation about the top, and (c) translation as a rigid body.

The type of wall movement is controlled by two variable-speed worm-gear drives. One operates on the upper driving rods and the other on the lower ones (see Fig. 2). For greater detail on the shaking table and its operation the reader is referred to Sherif, et. al. (Ref. 7 and 8).

4. Data Acquisition System

Due to the considerable amount of data that is generated from the shaking table experiments, a high-speed data acquisition system is used. The analog signal from the sensors is taken at a predetermined sample rate, and is then digitized by an Analog-to-Digital converter. The digital data are stored and processed by a PDP-11 mini-computer. The final data are printed digitally by a line printer and displayed in an analog form by a digital plotter.

## III. SOIL TYPE

Air-dry Ottawa silica sand was used throughout this investigation. The typical properties of the above soil are shown in Table 1 below.

Table 1. Soil Properties

| $D_{10}$, mm | $D_{30}$, mm | $D_{50}$, mm | $D_{60}$, mm | $C_u$ | $G_s$ | $e_{max}$ | $e_{min}$ |
|---|---|---|---|---|---|---|---|
| 0.18 | 0.22 | 0.25 | 0.26 | 1.50 | 2.67 | 0.75 | 0.53 |

## IV. TEST PROCEDURE

All tests during this study were conducted on the above soil at an average density of 102 pcf. This density was achieved by pouring the soil gently into the shaking table through a flexible tube and vibrating it at 6 Hz. frequency for 3 minutes under 0.45 g. At the end of the 3 minutes, acceleration levels of 0.00, 0.06g, 0.12g, 0.21g, 0.33g, 0.43g, and 0.57g were applied at 3.5 Hz. frequency while the retaining wall was rotated at a constant speed of $1.68 \times 10^{-4}$ rad/sec about the base. The stresses exerted against the retaining wall were measured by the stress transducers as a function of wall rotation. Typical data obtained during this process is shown in Fig. 4.

## V. ANALYSIS OF TEST RESULTS AND RECOMMENDATIONS FOR DESIGN

A. Test Results

Figure 4 shows variation of the horizontal pressures exhibited by pressure transducers SP1 through SP5 as a function of wall rotation about the base. It is clear from the data that there is an initial, abrupt drop in the horizontal stress values recorded by the transducers up to a certain wall rotation level, that the rate of stress reduction with further rotation decreases, and that eventually, a state of stress is reached whereby almost no reduction in stress value is observed with further wall rotation. Data from transducer SP1, a typical representation of which is provided in Fig. 5, shows the phenomenon.

This almost contstant stress level is defined as the dynamic active state of stress $\sigma_{AE}$.

Figure 6 shows the summary of the experimental total dynamic active stresses against the retaining wall as a function of acceleration levels ranging from 0.00 to 0.57g. On the basis of the presented data in Fig. 6, the following conclusions can be drawn about the stress distribution behind a rigid wall rotating about its base.

1. When no dynamic stresses are applied ($k_h = 0$), the active stress distribution behind the wall is linear up to about 80% of the wall height and is in conformity with the Coulomb and Mononobe-Okabe predictions. At lower depths, however, the stress distribution becomes non-linear and increases to the value of the static at-rest stress condition at the base (see point 1 in Fig. 6).
2. As the acceleration levels increase, the non-linearity in the stress distribution also increases, and it appears that unusually high stress values develop near the top of the backfill. These high stresses at the top may be explained in light of the differences between the shear strength of the soil and the dynamic inertia forces introduced by shaking. Since the granular soil at or near the surface have very little strength, its lateral stress transmission characteristics would therefore be higher than the soil at greater depths. This may explain why the unusual high stresses are observed near the top of the backfill during dynamic excitation. The stress magnitudes at the top of the backfill represented by points A, B, C and D in Fig. 6 were calculated by equating the values of the total thrust determined from the load cell readings with those from the total stress area obtained from pressure transducers. Points 2, 3, 4 and 5 in Fig. 6 correspond to the dynamic at-rest stress values.
3. The points of application of the total dynamic thrust increases with increasing accelerations in a non-linear fashion as shown in Fig. 7.

B. Design Recommendation and Illustrative Example

To translate the experimental findings into practical design principles, a series of stress design curves such as the ones in Fig. 8 is developed as a function of acceleration levels. These curves should enable the design engineer to determine the magnitudes of total dynamic active stresses $\sigma_{AE}$ at any depth behind the rotating wall when soil density and horizontal acceleration levels are known.

Illustrative Example

A granular soil behind a 10 ft-high rigid retaining wall has an average compacted density of 110 pcf. Determine the total dynamic active stress distribution behind the wall under a horizontal acceleration of 0.33g assuming that the wall rotates about its base.

To solve this problem, the values of the Dynamic Active Influence Factor $N_{AE}$ corresponding to 0.33g horizontal acceleration and 110 pcf soil density is found from Fig. 8 for any assumed value of z/H. Knowing the value of $N_{AE}$, the dynamic active stress distribution behind the above wall rotating about

its base can be obtained from the following equation where $\gamma$ is the soil density and H is the total wall height.

$$(\sigma_{AE})_{max.} = N_{AE}\ \gamma\ H = N_{AE}\ (110)\ (10)$$

ACKNOWLEDGEMENT

The authors gratefully acknowledge the financial supports of the National Science Foundation which made this investigation possible.

REFERENCES

1. Jokovlev, P.I., "Coefficient of Active and Passive Pressure on Retaining Walls under Seismic Conditions," Proceedings, Sixth World Conference on Earthquake Engineering, New Delhi, India, Vol. 3, 1977, pp. 2356-2362.
2. Matsuo, H. and Ohara, S., "Lateral Earth Pressures and Stability on Quay Walls during Earthquakes," Proceedings, Second World Conference on Earthquake Engineering, Japan, Vol. 1, 1960, pp. 165-181.
3. Ohara, S., "Experimental Studies of Seismic Active and Seismic Passive Earth Pressures," Proceedings, Third Japanese Earthquake Engineering Symposium, Tokyo, Japan, 1970, pp. 137-145.
4. Richards, R. and Elms, D., "Seismic Behavior of Gravity Retaining Walls," Journal of the Geotechnical Engineering Division, ASCE, Vol. 105, No. GT4, April 1979.
5. Scott, R.F., "Earthquake-Induced Earth Pressures on Retaining Walls," Fifth World Conference on Earthquake Engineering, Rome, Italy, Vol. 2, 1973, pp. 1611-1620.
6. Seed, H.B. and Whitman, R.V., "Design of Earth Retaining Structures for Dynamic Loads," Proceedings, ASCE Specialty Conference on Lateral Stresses in the Ground and the Design of Earth Retaining Structures, Cornell University, Ithaca, New York, June 1970.
7. Sherif, M.A., Ishibashi, I. and Lee, C.D., "Dynamic Earth Pressure against Retaining Structures," Soil Engineering Research Report No. 21, University of Washington, Seattle, 1981.
8. Sherif, M.A., Ishibashi, I. and Lee, C.D., "Earth Pressure against Rigid Retaining Walls," Journal of the Geotechnical Engineering Division, ASCE, Vol. 108, No. GT5, May 1982.
9. Wood, J.H., "Earthquake-Induced Soil Pressures on Structures," Report No. EERL 73-05, Earthquake Engineering Research Laboratory, California Institute of Technology, Pasadena, 1973.

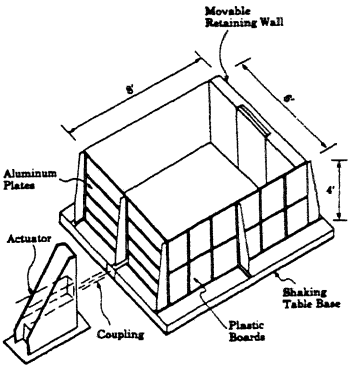


Fig. 1. Shaking Table, Soil Box, and Actuator Assembly.

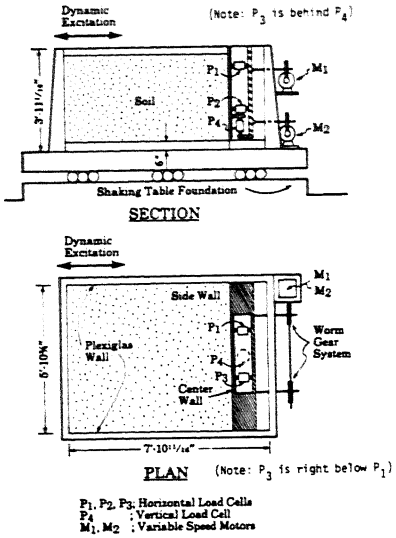


Fig. 2. Shaking Table with Movable Retaining Wall.

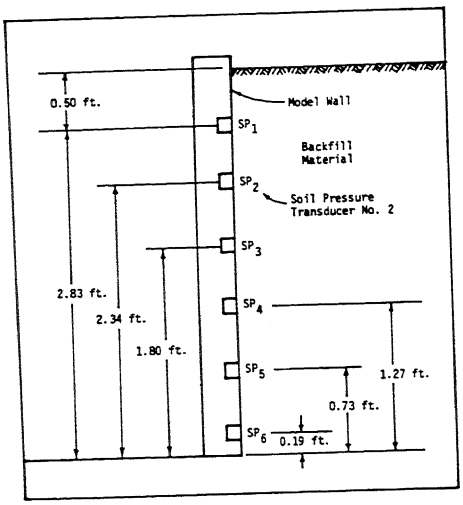


Fig. 3. Locations of Earth Pressure Transducers Behind the Rigid Center Wall.

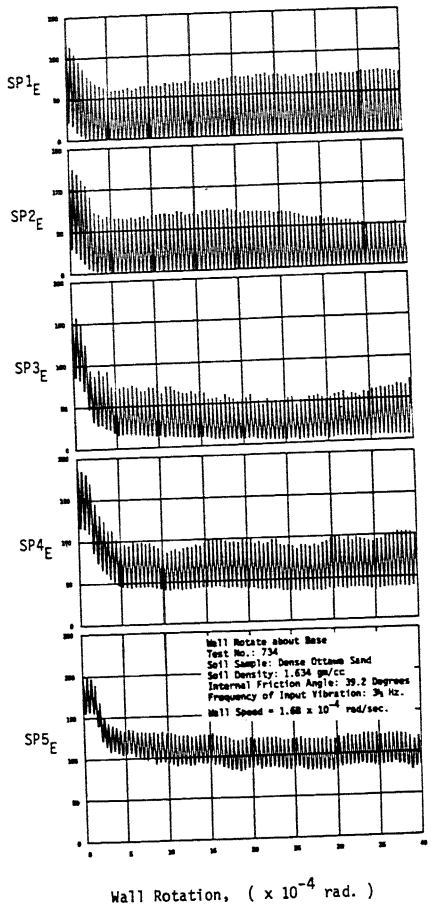


Fig. 4. Typical Dynamic Horizontal Pressures vs. Wall Rotation.

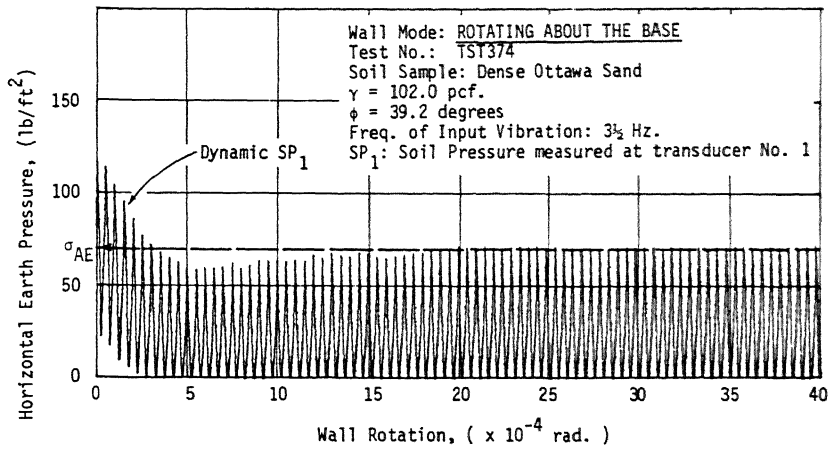


Fig. 5. Dynamic Earth Pressure Decrease as a Function of Wall Rotation and Definition of Dynamic Active Stress $\sigma_{AE}$.

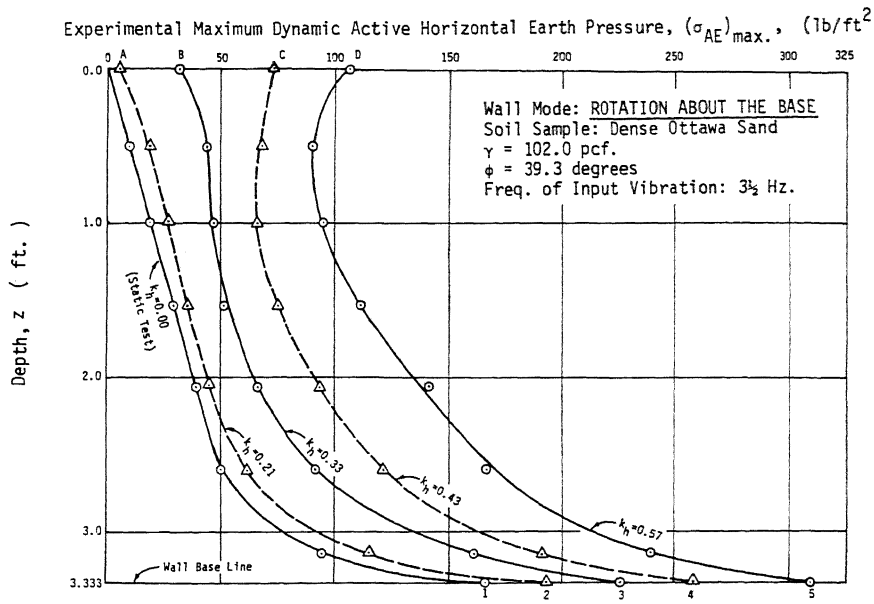


Fig. 6. Distribution of Maximum Dynamic Active Stresses behind a Rigid Wall Rotating about the Base as a Function of Horizontal Accelerations.

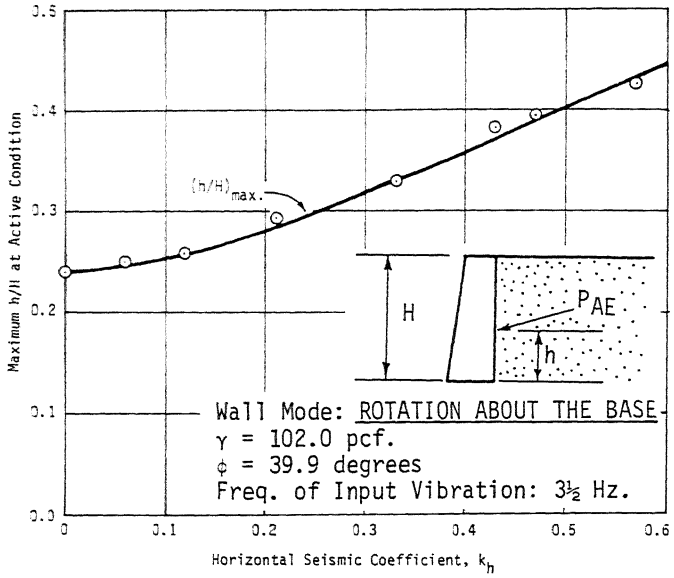


Fig. 7. Point of Application h/H of the Total Dynamic Active Thrust Versus Horizontal Acceleration.

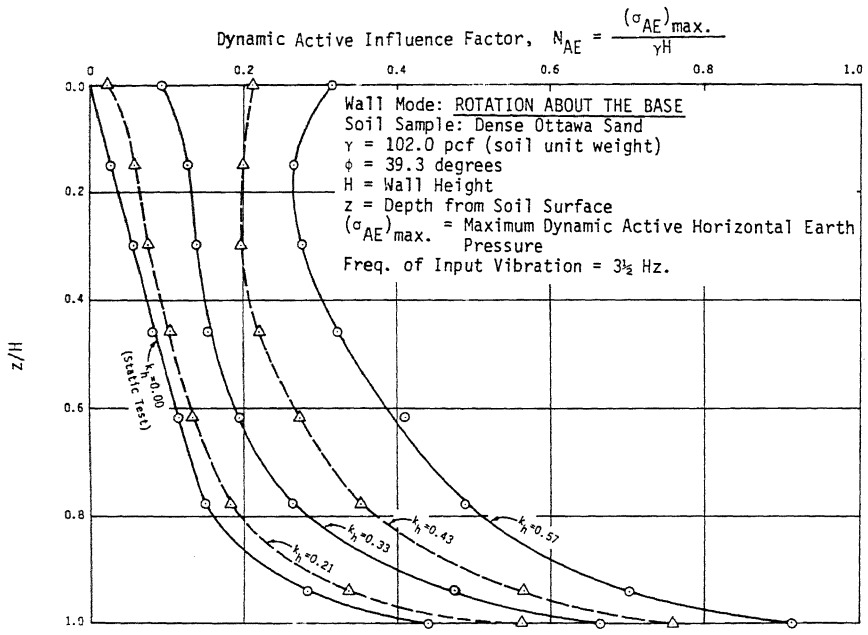


Fig. 8. Influence Factors for Maximum Dynamic Active Pressures behind a Rigid Wall Rotating about the Base as a Function of Horizontal Accelerations.